

A novel multifunctional electronic calibration kit integrated by MEMS SPDT switches

Shan-Shan Wang(王姗姗), Qian-Nan Wu(吴倩楠), Yue-Sheng Gao(高跃升), Jian-Gang Yu(余建刚), Qian-Long Cao(曹钎龙), Lu-Lu Han(韩路路), and Meng-Wei Li(李孟委)

Citation: Chin. Phys. B, 2021, 30 (**11**): 118501. DOI: 10.1088/1674-1056/abf12b
Journal homepage: http://cpb.iphy.ac.cn; http://iopscience.iop.org/cpb

What follows is a list of articles you may be interested in

Reversible waveform conversion between microwave and optical fields in a hybrid opto-electromechanical system

Li-Guo Qin(秦立国), Zhong-Yang Wang(王中阳), Jie-Hui Huang(黄接辉), Li-Jun Tian(田立君), and Shang-Qing Gong(龚尚庆)

Chin. Phys. B, 2021, 30 (**6**): 068502. DOI: 10.1088/1674-1056/abea8f

Opto-electromechanically induced transparency in a hybrid opto-electromechanical system

Hui Liu(刘慧), Li-Guo Qin(秦立国), Li-Jun Tian(田立君), Hong-Yang Ma(马鸿洋)

Chin. Phys. B, 2019, 28 (**10**): 108502. DOI: 10.1088/1674-1056/ab3af2

Efficient molecular model for squeeze-film damping in rarefied air

Cun-Hao Lu(陆存豪), Pu Li(李普), Yu-Ming Fang(方玉明)

Chin. Phys. B, 2019, 28 (**9**): 098501. DOI: 10.1088/1674-1056/ab3443

Electrically controlled optical switch in the hybrid opto-electromechanical system

Li-Guo Qin(秦立国), Zhong-Yang Wang(王中阳), Hong-Yang Ma(马鸿洋), Shu-Mei Wang(王淑梅), Shang-Qing Gong(龚尚庆)

Chin. Phys. B, 2017, 26 (**12**): 128502. DOI: 10.1088/1674-1056/26/12/128502

Excellent ethanol sensing properties based on Er_2O_3-Fe_2O_3 nanotubes

Liu Chang-Bai, He Ying, Wang Sheng-Lei

Chin. Phys. B, 2015, 24 (**11**): 118501. DOI: 10.1088/1674-1056/24/11/118501

A novel multifunctional electronic calibration kit integrated by MEMS SPDT switches*

Shan-Shan Wang(王姗姗)[1,2,3,4], Qian-Nan Wu(吴倩楠)[2,3,4,5,†], Yue-Sheng Gao(高跃升)[1,2,3,4], Jian-Gang Yu(余建刚)[1,2,3,4], Qian-Long Cao(曹钎龙)[1,2,3,4], Lu-Lu Han(韩路路)[1,2,3,4], and Meng-Wei Li(李孟委)[1,2,3,4,‡]

[1] *School of Instrument and Electronics, North University of China, Taiyuan* 030051, *China*
[2] *Nantong Institute of Intelligent Opto-Mechatronics, North University of China, Nantong* 226000, *China*
[3] *Center for Microsystem Intergration, North University of China, Taiyuan* 030051, *China*
[4] *Academy for Advanced Interdisciplinary Research, North University of China, Taiyuan* 030051, *China*
[5] *School of Science, North University of China, Taiyuan* 030051, *China*

(Received 20 February 2021; revised manuscript received 15 March 2021; accepted manuscript online 24 March 2021)

Design and simulation results of a novel multifunctional electronic calibration kit based on microelectromechanical system (MEMS) single-pole double-throw (SPDT) switches are presented in this paper. The short-open-load-through (SOLT) calibration states can be completed simultaneously by using the MEMS electronic calibration, and the electronic calibrator can be reused 10^6 times. The simulation results show that this novel electronic calibration can be used in a frequency range of 0.1 GHz–20 GHz, the return loss is less than 0.18 dB and 0.035 dB in short-circuit and open-circuit states, respectively, and the insertion loss in through (thru) state is less than 0.27 dB. On the other hand, the size of this novel calibration kit is only 6 mm×2.8 mm×0.8 mm. Our results demonstrate that the calibrator with integrated radio-frequency microelectromechanical system (RF MEMS) switches can not only provide reduced size, loss, and calibration cost compared with traditional calibration kit but also improves the calibration accuracy and efficiency. It has great potential applications in millimeter-wave measurement and testing technologies, such as device testing, vector network analyzers, and RF probe stations.

Keywords: microelectromechanical system (MEMS), electronic calibration kit, single-pole double-throw (SPDT) switch, short-open-load-through (SOLT) calibration

PACS: 85.85.+j, 87.80.Ek **DOI:** 10.1088/1674-1056/abf12b

1. Introduction

With the rapid development of electronics, medicine, industries, automotive, and aerospace technology, the requirements for miniaturization and high reliability of systems are increasing, and these requirements can be fundamentally achieved by high-degree integration of systems. The microelectromechanical system (MEMS) technology has gained popularity in the electronic information field, such as in the fabrication of integrated circuits, to produce miniaturized, intelligent, and integrated MEMS devices. At present, devices based on MEMS technology have gradually moved from the laboratory to practical application level, and they greatly contribute to the development of fields such as industry and agriculture, information, environment, bioengineering, medical treatment, space technology, and national defense.[1–4] The MEMS-based devic12-es such as radio-frequency microelectromechanical system (RF MEMS) switches,[5–7] attenuators,[8,9] filters,[10,11] and phase shifters[12–15] have been developed. However, the network analyzer, microwave test cable, and load used in the RF performance testing process all encounter problems of large loss, instability, and non-repeatability, and these problems directly result in the low accuracy of MEMS device testing.[16–18] Therefore, the test cable, load, test instrument, and other systems need calibrating prior to the MEMS device testing in order to minimize the system errors generated during the test, thereby improving the measurement accuracy of the MEMS device.[19]

Currently, most widely used calibration kits for MEMS devices are mechanical[20,21] and electronic[22] calibration kits, based on the coaxial calibration principle. Mechanical calibration kits are easy to operate and have high dependency on operator skills, whereas electronic calibration kits use automated operation, which is fast and less affected by operator skills. However, for the calibration of non-coaxial MEMS devices, both calibration kits encounter the problems of low matching degree and high error rate. In response to this, a through-reflect-line (TRL) calibration kit for S-parameter characterization of membrane circuits for the WR-03 waveguide band (220 GHz–325 GHz) was developed at Chalmers

*Project supported by the National Defense Technology Industry Strong Foundation Project, China (Grant No. JCKY2018408B006), the Information System New Items Project, China (Grant Nos. 2018XW0026 and 2019XW0010), and the Information System Pre-research Project, China (Grant No. 31513060101).

†Corresponding author. E-mail: qiannanwoo@nuc.edu.cn
‡Corresponding author. E-mail: lmwnuc@163.com

© 2021 Chinese Physical Society and IOP Publishing Ltd

University of Technology.[23] Testing results verified that the calibrator has good response characteristics and reliability, but low sensitivity. A printed circuit board (PCB) was used to design and produce an electronic calibration kit suitable for power amplifiers (PA) at Malaysian University of Science and Technology.[24] Although the measurement accuracy of this calibration system was approximately 10% higher than that of traditional calibration kits, its size was at least six times larger than that of a sub-miniature A (SMA) interface connector. A non-contact detection calibration kit for 220 GHz–325 GHz was designed and produced at Ohio State University,[25] which effectively improves the mismatch caused by the wear of the probe tip. However, its operation is complicated and requires human operator judgment, which greatly affects the repeatability of the calibration kit.

To address the above-mentioned problems associated with existing MEMS device calibration methods, in this study a multifunctional electronic calibration kit is proposed and designed by using cascaded MEMS-based SPDT switches. The SOLT calibration states can be completed simultaneously, and the metallization of probe tip and errors introduced by human operation can be reduced by using the MEMS electronic calibration. It can calibrate a vector network analyzer, microwave probe station, and test cable in a frequency range of 0.1 GHz–20 GHz with high precision, and the overall size of this novel proposed calibrator kit is only 6 mm×2.8 mm×0.8 mm.

2. Theory

At present, the most effective and direct testing method of RF parameters of MEMS devices in the millimeter wave band is to use a vector network analyzer, a microwave probe station, a test cable, and a test method for connecting the device under test. The loss introduced by the cable and the probe will directly result in inaccurate test results. The commonly used two-port calibration methods are SOLT and TRL (straight-reflect-reflection line).[26] The SOLT calibration kit is easy to operate, and can provide excellent accuracy and repeatability, so it is more commonly used. Figure 1(a) shows the calibration kit for a probe station. The ground wire–signal wire–ground wire (GSG) probe is directly calibrated on a calibration sheet on which the short-circuit, open-circuit, load, and through (thru) units are arranged and distributed as shown in Fig. 1(b). In the dual-port calibration process performed by the vector network analyzer, the GSG probes connected to the port of the mobile network analyzer calibrate short-circuit, open-circuit, and load at ports 1 and 2; then, the two probes are placed on the thru calibration unit simultaneously. The four calibration units are immersed in sequence seven times to measure the S-parameters; subsequently, 12 errors are calculated according to the SOLT calibration formula. Thus, the calibration of the vector network and the probe station are completed.[27,28] The functions of the calibration ports are as follows.

Short calibration: The signal achieves an ideal short circuit on the calibration kits (total reflection $|\Gamma| = 1$) and undergoes total reflection, yielding return loss S_{11} close to 0.

Open calibration: The signal achieves an ideal open circuit (total reflection $|\Gamma| = 1$) on the calibration kit and undergoes total reflection, yielding return loss S_{11} close to 0.

Load calibration: The signal realizes an accurate broadband impedance matching with the system impedance on the calibration kit.

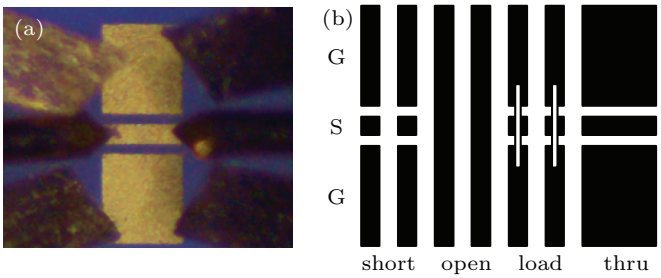


Fig. 1. (a) Thru calibration of probe, and (b) calibration on-chip calibration kits.

2.1. Design of electronic calibration kit

The RF MEMS devices have characteristics of small size, low loss, and easy integration, and have important applications in the development of miniature, intelligent, light-weight, and low-power-consumption communication systems.[29] Compared with traditional electronic switches, RF MEMS switches have high frequency, small size, low power consumption, and high-degree integration, and they are used in many electronic devices. In this study is proposed an RF MEMS switch that can be introduced into an electronic calibration kit to realize a small-volume, low-loss, convenient, and multifunctional integrated electronic calibration kit as shown in Fig. 2. The calibration kit consists of a standard short-circuit port Z_0, a standard open port Z_1, and a standard load port Z_2.

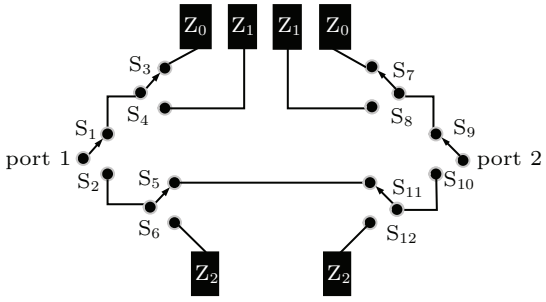


Fig. 2. Overall scheme of calibration kit.

The signal from port 1 passes through switches S_1 and S_3 and enters into Z_0, providing the short-circuit calibration of port 1. The signal from port 2 passes through switches S_9 and S_7 to reach Z_0, providing the short-circuit calibration of port 2. The signal from port 1 passes through switches S_1 and S_4 to arrive at Z_1, providing the open calibration of port

1. The signal from port 2 enters into switches S_9 and S_8 and reaches Z_1, realizing the open calibration of port 2. The signal from port 1 enters into switches S_2 and S_6 and reaches Z_2, realizing the load calibration of port 1. The signal from port 2 enters into switches S_{10} and S_{12} and reaches Z_2, providing the load calibration of port 2. Finally, the signal enters into switches S_2, S_5, S_{11}, and S_{10} from port 1 to port 2, which can be directly calibrated to complete the network signal dual-port calibration. This calibration kit is thus simple and convenient.

2.2. Design and simulation of RF MEMS SPDT switch

The RF MEMS SPDT switch is a three-port structure in which signals are input from one port and output to either of the other two ports selectively. The signal is input from the input port and is divided into two channels for transmission by the T-type power divider, and each channel has an RF MEMS switch. By controlling the opening or closing of the RF MEMS switch of each channel, the selected output of signal is realized.

Figure 3 is a schematic diagram of the typical series contact RF MEMS SPDT switch. When sufficient driving voltage is applied between the upper plate and lower plate of the RF MEMS switch, the upper electrode will move vertically downward under the action of electrostatic force, and the signal is turned on and the switch is closed as shown on port 2. When the driving voltage between the upper plate and lower plate is removed, the upper electrode is restored to the original position under the action of the restoring force, the signal is disconnected, and the switch is in the disconnected state as shown in port 3.

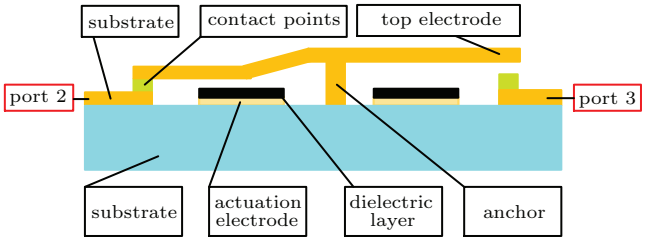


Fig. 3. Schematic diagram of RF MEMS SPDT switch.

To meet the requirements for the application of the standard calibration kit, the ADS software is used to calculate the basic physical dimensions of the substrate and coplanar waveguide at a matching impedance of 50 Ω. In this study is adopted a series contact-type MEMS SPDT switches in the electrostatic drive mode, and the upper electrode has a simple straight-plate structure. It is composed of a glass substrate (dielectric constant is 4.6, thickness is 500 μm), a coplanar waveguide reflection line (20 μm/120 μm/20 μm), a straight-plate-type top electrode, an actuation electrode, air bridges, a contact point, and a driver. The electrodes and other kit are shown in Fig. 4.

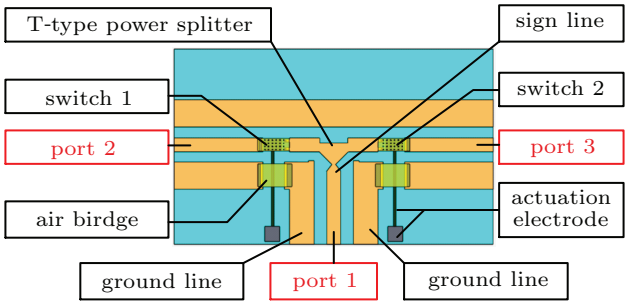


Fig. 4. Structure of SPDT switch.

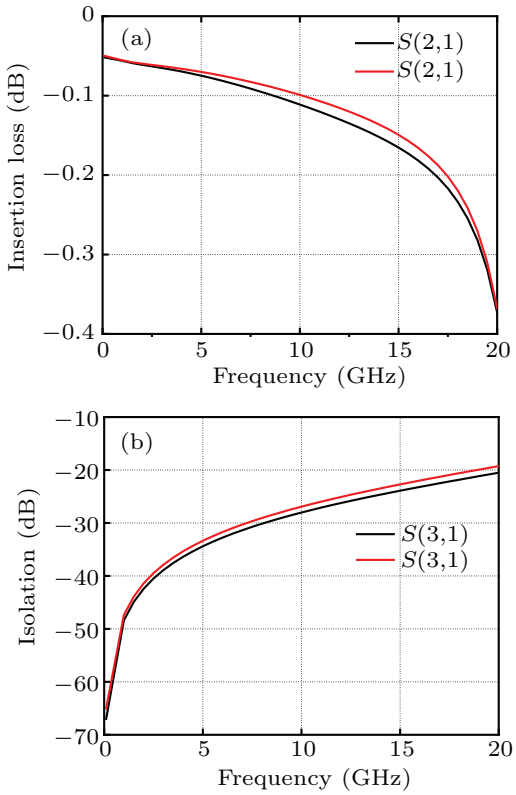


Fig. 5. (a) Insertion loss and (b) isolation of SPDT switch.

The results of the simulation conducted by using the ANSOFT HFSS software are shown in Fig. 5. When the input signal enters into port 1, the insertion loss is 0.36 dB at 20 GHz through port 2, with isolation 20 dB at 20 GHz, and the insertion loss is 0.37 dB at 20 GHz through port 3, with isolation 21.83 dB at 20 GHz. The results indicate that the two ports of the designed RF MEMS SPDT switch have good insertion loss and isolation, and excellent consistency with each other as well.

2.3. Design of load resistance

The load resistance is an important factor and should be considered in calibration under a load state. In this study, a tantalum nitride thin-film resistor with self-passivation, high corrosion resistance, and high stability is selected in the design.[30] The resistance of the thin-film resistor is related to its size and geometry and can be calculated from

$$R = R_0 \times \frac{l}{w},$$

where R_0 is the square resistance of the thin-film resistor (100 Ω/□ tantalum nitride resistor is selected in this study), l is the length of the thin-film resistor (50 μm), and w is the width of the thin-film resistor (100 μm).

The ANSOFT HFSS software is used to simulate a 50-Ω load resistance, and the simulation results are shown in Fig. 6. At 0.1 GHz–20 GHz, the return loss is within 10.95 dB–11.07 dB. The resistor has good stability and can be used as a load standard for calibration.

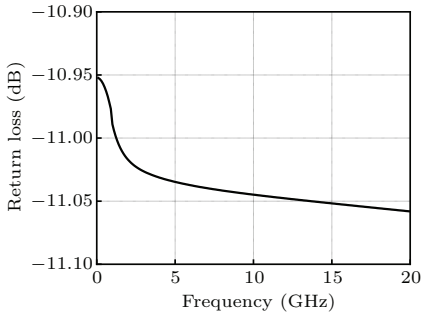


Fig. 6. Simulation results of load resistance.

2.4. Design of electronic calibration kit based on RF SPDT switch

Figure 7 shows the structure of the entire electronic calibration kit, which is composed of symmetrically cascading five RF MEMS SPDT switches. For the vector network analyzer to perform single-port calibration, three calibrations are required. First, port 1 probe of the vector network analyzer port contacts port 1, and switches 1–4 are all open at the same time. the calibration kit is in a short-circuit state, and single-ended short-circuit calibration is performed. Control switches 1 and 3 are both open. Next, switch 5 is switched off and the calibration kit is in the open state, then single-ended open circuit calibration is performed. Control switches 1, 3, 5, and 6 are all open, the calibration kit is in load resistance state, and 50-Ω load calibration is performed. For the single-ended calibration by the vector network analyzer, the calibration is performed seven times. The switch status is shown in Table 1. The vector network analyzer ports CH 1 and CH 2 contact port 1 and port 2 of the calibrator, respectively. Then, the two ports are calibrated in the states of shorted circuit, open circuit, load, and thru by closing the control switches. This process requires only two probe contacts, thus reducing the effect of human errors on the calibration accuracy.

The switch status of each calibration state is shown in Table 1, where 1 indicates that the switch is on and 0 represents that the switch is off.

The ANSOFT HFSS software is used to simulate the RF performance of the electronic calibration kit based on the MEMS SPDT switch, and the simulation results are shown in Fig. 8. Figure 8(a) shows the return loss of the calibration kit in the short-circuit state. Figure 8(b) indicates the return loss of the calibration kit in the open-circuit state. Figure 8(c) displays the return loss of the calibration kit in the load-circuit state, and figure 8(d) exhibits the insertion loss in the thru state.

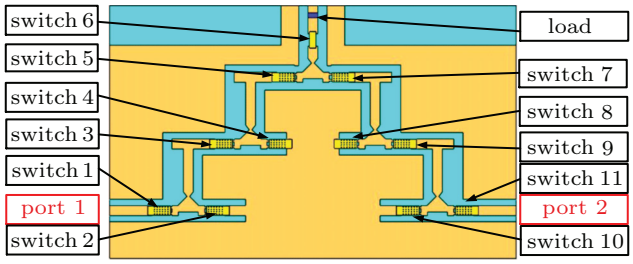


Fig. 7. Structure of electronic calibration kit based on RF SPDT switch.

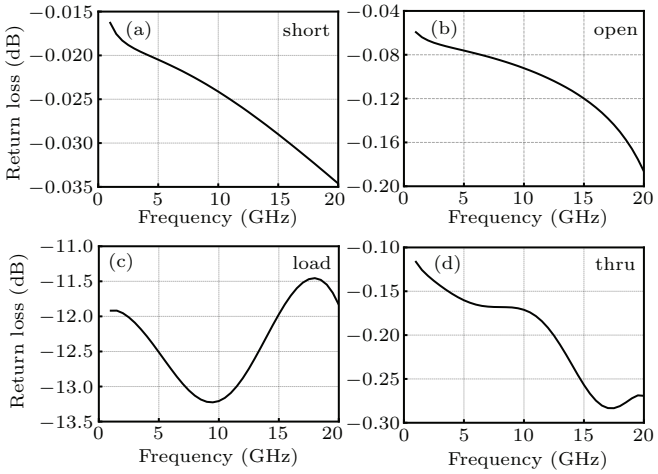


Fig. 8. Simulation results of calibration kit: return loss in (a) short state, (b) open state, and (c) load state, and (d) insertion loss in thru state.

Table 1. Corresponding switch mode of calibration state.

Switch	S1	S2	S3	S4	S5	S6	S7	S8	S9	S10	S11
Short 1	1	1	1	1	0	0	0	0	0	0	0
Short 2	0	0	0	0	0	0	0	1	1	1	1
Open 1	0	0	0	0	0	0	0	0	0	0	0
Open 2	0	0	0	0	0	0	0	0	0	0	0
Load 1	1	0	1	0	1	1	0	0	0	0	0
Load 2	0	0	0	0	0	1	1	0	1	0	1
Thru	1	0	1	0	1	0	1	0	1	0	1

The simulation results indicate that for a frequency range of 0.1 GHz–20 GHz, the electronic calibrator can be reused and needs only two steps for one-time calibration. Further, the return loss is less than 0.18 dB in the short-circuit state is less than 0.18 dB and less than 0.035 dB in the open-circuit state. This suggests a lower reflection error. When the load resistance is 50 Ω, the echo is within 11.5 dB–13.5 dB, showing good stability. In the thru state, the insertion loss less than 0.27 dB has a lower reflection error. This calibration kit exhibits an excellent performance during dual-port calibration.

3. Fabrication and measurement of SPDT switch

In order to verify the simulation results of this novel multifunctional electronic calibration kit, the core device of the

RF MEMS SPDT switch is fabricated by micro-nano surface technology,[31] and the fabrication process consists of nine steps and is shown in Fig. 9.

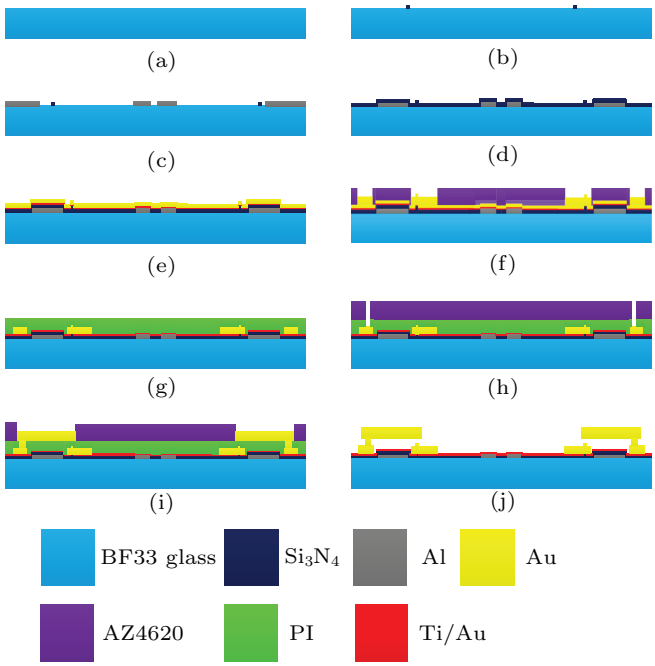


Fig. 9. Fabrication processes of SPDT switch.

Step (a) The surface of the BF33 glass sheet is cleaned to remove various inorganic impurities and organic contaminants.

Step (b) A 400-nm-thick silicon nitride film layer is deposited by PECVD at 350 °C, and dry etching is performed to obtain bumps contacting the ohmic series switch.

Step (c) A 500-nm-thick aluminum film layer is deposited by magnetron sputtering and the wet etching is performed by using concentrated phosphoric acid to obtain the driving electrode and PAD of SPDT.

Step (d) A 300-nm-thick silicon nitride film layer is deposited again by PECVD, servins as an isolation layer, which is used to prevent metal-to-metal contact from diffusing and also to prevent aluminum metal from being destroyed by subsequent processes.

Step (e) A 50-nm-thick titanium adhesion film layer is deposited on the isolation layer, followed by a 150-nm-thick gold layer. The purpose of Ti/Au metal layer is to serve as a seed layer for electroplating coplanar waveguide (CPW).

Step (f) A 2-μm-thick Au layer is selectively deposited as CPW, and the Au layer also covers the exposed contact points of the series ohmic switches to provide low contact resistance.

Step (g) A Ti/Au seed layer is then removed by wet etching. Finally, the isolation nitride spacer is defined by photolithography and dry etching to expose the underlying PAD. The over-etch time of dry etching is determined by considering the removal of Si_3N_4 capping and exposure of the underlying aluminium layer. The sacrificial layer for the definition of air gap is formed by 4-μm thick polyimide (PI). In order to solve the problem of PI step coverage, the spin-coated PI wafer is horizontally placed in a covered petri dish, and then the petri dish is placed in an oven at a constant temperature of 50 °C for 4 h. The temperature and time parameters are selected based on the fact that the liquid PI has the fastest flow rate at 50 °C and will become solid after 4 h, so 50 °C and 4 h are chosen.

Step (h) The anchor vias in the sacrificial layer are obtained by a mask and wet etching, and followed closely by the alkaline developer dissolving the upper photoresist and continuing to etch the underlying PI.

Step (i) The beams of the switches and the air bridges are formed when a 2-μm-thick gold layer is electroplated. Then the seed layer is removed by wet etching.

Step (j) The sacrificial layer is released. At this point the manufacturing process of the switch is completed. The scanning electron microscopy (SEM) image of the prepared SPDT switch is shown in Fig. 10.

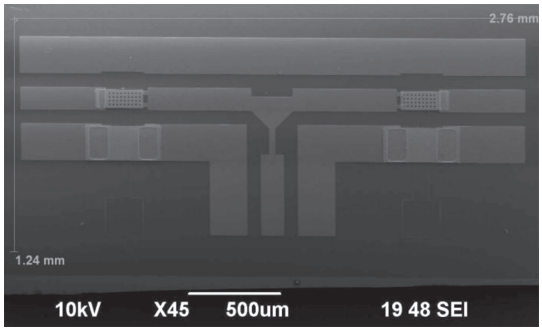


Fig. 10. SEM photograph of SPDT switch.

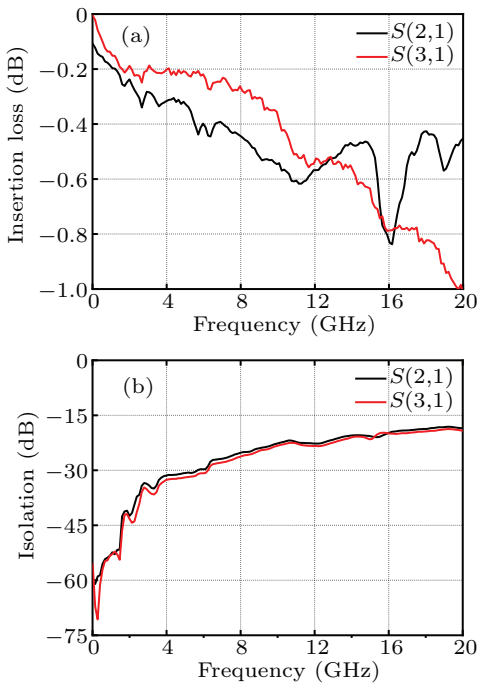


Fig. 11. (a) Measured insertion loss response of SPDT switch, and (b) measured isolation response of SPDT switch.

The test results are shown in Fig. 11, which shows that the insertion loss of the MEMS SPDT switch is less than 1.0 dB and the isolation is more than 18 dB, which satisfies the design specifications and calibration requirements. The calibration sheet used for the probe can be used only once, whereas the MEMS SPDT switch prepared in this study can be used 10^6 times; the insertion loss changes after multiple tests has become small and the repeatability is good. The measurements and the simulations accord well each other, which makes the process and technology of designing multifunctional electronic calibration kit more confident.

4. Conclusions and perspectives

The electronic calibration kit in four calibration states are proposed that is composed of the five cascaded MEMS SPDT switches and one load resistance. In the working frequency band of 0.1 GHz–20 GHz, the return loss of the calibration kit is less than 0.18 dB in the shorted circuit state and less than 0.035 dB in the open circuit state, the insertion loss is less than 0.27 dB in the thru state. The electronic calibrator can be reused 10^6 times and needs only two steps for one-time calibration. The calibration method has addressed the problems of the traditional calibration with a single function and many cumbersome calibration steps. Therefore, the multifunctional calibration kit can provide a convenient calibration method for the microwave test systems, such as vector network analyzers, RF probe stations, and millimeter wave test cables.

Acknowledgment

We thank the Key Laboratory of Instrumentation Science and Dynamic Measurement for their technique support.

References

[1] Mishra M K, Dubey V, Mishra P M and Khan I 2019 *Journal of Engineering Research and Reports* **4** 1
[2] Yao B Y, Feng L S, Wang X, Liu W F and Liu M H 2014 *Chin. Phys. Lett.* **31** 078501
[3] Yao B Y, Zhou Z, Feng L S, Wang W P and Wang X 2012 *Chin. Phys. Lett.* **29** 118502
[4] Zhang Z H, Ren T L, Zhang Y H, Han R Rand Liu L T 2012 *Chin. Phys. Lett.* **29** 088501
[5] Li M, Zhao J, You Z and Zhao G 2017 *Solid-State Electron.* **127** 32
[6] Qin L G, Wang Z Y, Ma H Y, Wang S M and Gong S Q 2017 *Chin. Phys. B* **26** 128502
[7] Li M, Liu Q, Wu Q, Wu Q and Han Y 2019 *Microsystem Technologies* **25** 1619
[8] Li M, Zhang Y, Zhao Y, Xue P and Wu Q 2020 *Analog Integrated Circuits and Signal Processing* **102** 617
[9] Guo X, Gong Z, Zhong Q, Liang X and Liu Z 2016 *Journal of Micromechanics and Microengineering* **26** 1
[10] Zacchini L, Calabro V, Candeloro, M, Fanelli F, Ridolfi A and Dukan F 2020 *IEEEASME Transactions on Mechatronics* **99** 1
[11] Campanella H, Qian Y, Romero C O, Giner J and Kumar R 2020 *IEEE 33rd International Conference on Micro Electro Mechanical Systems*, January 18–22, 2020, Vancouver, British Columbia, Canada, pp. 218–221
[12] Edinger P, Errando-Herranz C and Gylfason K B 2019 *IEEE 32nd International Conference on Micro-Electro-Mechanical Systems*, January 27–31, 2019, Seoul, Korea, pp. 919–921
[13] Ravani K G, Guha K and Rao K S 2020 *Int. J. Electron.* **107** 1822
[14] Han J and Liao X 2016 *IEEE Sensors*, October 30–November 3, 2016, Orlando, FL, USA, pp. 1–3
[15] Dey S, Koul S K, Poddar A K and Rohde U 2020 *ISSS Journal of Micro and Smart Systems* **9** 33
[16] Stumper U 2002 *Conference Digest Conference on Precision Electromagnetic Measurements*, June 21–21, 2002, Ottawa, Ont., Canada, pp. 132–133
[17] Khankalantary S, Ranjbaran S and Ebadollahi S 2021 *Measurement Science and Technology* **32** 045102
[18] Stumper U 2005 *IEEE Transactions on Instrumentation and Measurement*, March 21, 2005, **54** 676
[19] Wu A, Liu C, Liang F, Zou X and Ridler N 2020 *IEEE Transactions on Microwave Theory and Techniques* **99** 1
[20] Silvonen K J 1992 *IEEE Transactions on Microwave Theory and Techniques* **40** 754
[21] Kishikawa R and Horibe M 2020 *Conference on Precision Electromagnetic Measurements (CPEM)*, August 24–28, 2020, Denver, CO, USA, pp. 1–4
[22] Zhu W and Han X D 2010 *Foreign Electronic Measurement Technology* **29** 082022 (in Chinese)
[23] Zhao H, Tang A Y, Sobis P, Bryllert T, Yhland K, Stenarson J and Stake J 2010 *35th International Conference on Infrared Millimeter, and Terahertz Waves*, September 5–10, 2010, Rome, Italy, pp. 1–2
[24] Hamid S S, Ain M F, Mohd S K K, Zawawi R A, Rhaffor N and Manaf A A 2016 *IEEE International Conference on Automatic Control and Intelligent Systems*, October 22, 2016, Selangor, Malaysia, pp. 147–150
[25] Sertel K 2019 *92nd ARFTG Microwave Measurement Conference*, January 20–23, 2019, Orlando, Florida, USA, pp. 1–4
[26] Safwat A M E and Hayden L 2001 *58th ARFTG Conference Digest*, November 29–30, 2001, San Diego, CA, USA, pp. 1–10
[27] Butler J V and Rytting D K 1991 *IEEE Transactions on Microwave Theory & Techniques* **39** 2211
[28] Luo W, Hu A, Liu K and Chen X 2016 *International Conference on Advanced Electronic Science and Technology*, August 19–21, 2016, Shenzhen, China, pp. 276–282
[29] Li M and Hu T 2021 *Defence Technology* **17** 450
[30] Koutsoureli M, Stavrinidis G, Birmpiliotis D, KonstantinidisG and Papaioannou G 2020 *Microelectronic Engineering* **223** 111230
[31] Bustillo J M, Howe R T and Muller R S 1998 *Proc. IEEE* **86** 1552